Energy Conversion and Management 105 (2015) 518–529

Contents lists available at ScienceDirect

Energy Conversion and Management

journal homepage: www.elsevier.com/locate/enconman

Timing optimization of single-stage single-acting reciprocating expansion engine based on exergy analysis

Mahmood Farzaneh-Gord, Mohsen Jannatabadi *

The Faculty of Mechanical Engineering, Shahrood University of Technology, Shahrood, Iran

ARTICLE INFO

Article history:
Received 23 April 2015
Accepted 4 August 2015
Available online 19 August 2015

Keywords:
Natural gas
Single acting expansion engine
Exergy efficiency
Genetic Algorithm
Timing optimization

ABSTRACT

For recovering the waste potential energy of natural gas during pressure reduction in City Gate Stations (CGS), Reciprocating Expansion Engine (REE) could be utilized instead of throttling valves. The main goal of this theoretical analysis is to optimize ports opening and closing time of REEs. The first and second law analysis of the natural gas inside the cylinder, as a control volume, has been carried out for optimization. The optimization is based on Genetic Algorithm from exergy efficiency concept. The influence of the REE pressure ratio on the exergy efficiency is analyzed by numerical calculations too. In general, the results of the analysis showed that exergy efficiency based on optimization of inlet/outlet ports opening and closing timing has a huge impact on the REE performance. It was found that for optimized timing, exergy destruction due to outlet throttling is two or three times of destruction due to inlet throttling, in one case 14.5 kW against of 6 kW. It is also found that engine size does not have much impact on the port timings. The results showed that exergy destruction due to mixing and heat transfer can be neglected, although friction and inlet/outlet throttling have a significant impact on exergy loss. The portion of friction is about 5–10% in all cases. It is also found that inlet pressure has significant effects on optimized port timing. In cases of inlet pressure of 70 bars, inlet processes should be finished at 63° and in cases of 55 bars it is about 72°. If a REE is optimized for inlet pressure of 70 bar, it should not be utilized for inlet pressure less than 30 bar.

1. Introduction

Natural Gas (NG) pressure should be reduced in City Gate stations (CGS) before its transmission for being consumed in local distribution systems. The expansion valve is traditionally used for pressure reduction. Expansion valve destroy a lot of potential energy of high pressure natural gas during pressure reduction. There are a lot of researches to analyze the methods for recovering this huge wasted energy. These methods consist of using combined heat and power (CHP) and turbo expanders [1–6]. Exergy recovery and energy analysis of pressurized gas in natural gas expansion plants by using of internal combustion engine (ICE) and an organic Rankine cycle (ORC) has been studied [7–9].

A few studies have been carried out on using turbo expanders instead of throttling valve to recover the wasted potential energy in natural gas pressure reduction [10–12]. Using of solar heating unit due to decreasing fuel consumption and installing turbo expander instead of throttling valve for power generation has been studied [13].

It has been shown that the amount of pressure drop is the main parameter which has a huge impact on the amount of power output. The effect of turbine's isentropic efficiency on power output has been analyzed too [10]. It has shown that the variation of flow rate has a significant effect on the amount of power generation [11]. Another investigation shows that installing turbo expander in parallel with expansion valve has financial benefit over a year [12].

There is a very good possibility of recovering energy from pressurized gas during pressure reduction using REE. Power generation from REE is clean and could be considered as green energy. A schematic diagram of a REE is shown in Fig. 1. Nowadays, employing natural gas reciprocating single or double acting expansion engine in parallel with expansion valve is getting a popular alternative option [14]. Single-acting REE (see Fig. 2) which could be made less expensive than double acting only has one expansion stroke per revolution of crankshaft. Therefore, the expansion of gas will take place on the top side of the piston. This means that the piston is only powered by gas on its down stroke and needs the momentum of the crankshaft to force it back up from Bottom Dead Center (BDC) to Top Dead Center (TDC).

Although REEs have been employed in NG industries for pressure reduction, there is a very limited research about these

* Corresponding author.
E-mail addresses: imchm@yahoo.co.uk (M. Farzaneh-Gord), m_jannatabadi@yahoo.com (M. Jannatabadi).

http://dx.doi.org/10.1016/j.enconman.2015.08.012
0196-8904/© 2015 Elsevier Ltd. All rights reserved.

Nomenclature

A	instantaneous heat transfer area (m^2)
$A_{s,d}$	inlet/outlet port area (m^2)
b	specific flow exergy function (kW)
C_L	clearance volume (m^3)
C_P	constant pressure specific heat (j/kg K)
C_V	constant volume specific heat (j/kg K)
D_i	piston diameter (m)
D_o	outside diameter (m)
E	energy (kW)
d	port diameter (m)
f	friction factor
h	specific enthalpy (j/kg)
$\dot{I}$	exergy destruction (kW)
L	connecting rod length (m)
t	time (s)
L_r	ring wide (m)
$\dot{m}$	mass flow rate (kg/s)
N	motor speed (rpm)
P	pressure (Pa)
$\dot{Q}$	heat transfer rate (kW)
R	crank radius (m)
R_g	constant coefficient of methane (j/kg K)
r_p	pressure ratio
$\dot{S}_{gen}$	entropy generation (W/K)
s	specific entropy (j/kg K)
T	temperature (K)
T_0	dead state temperature (K)
T_a	ambient temperature (K)
u	internal energy (j/kg)
U	overall heat transfer coefficient (w/m^2 K)
V	volume (m^3)
W	power (kW)
x	piston displacement (m)
γ	isentropic power
Ψ	exergy efficiency
θ	instant angle of connecting rod (°)
$\dot{\Xi}$	rate of exergy transfer (kW)
ω	rotational speed (rad/s)

Subscripts

av	average
0	clearance volume
b	brake work
c	control volume of expansion engine
d	discharge
dis	cylinder volume
f	friction
i	identifier for inlet flow stream
id	ideal
ind	indicator
in	inside cylinder
mix	refer to mixing
out	outside cylinder
Q	refer to heat transfer
r	ring piston
s	suction
t	total exergy transfer
th	refer to throttling
w	wall cylinder

engines. One report shows that the amount of power generation by REE from natural gas potential energy depends on mass flow rate, pressure ratio and NG preheating [14]. Since experimental investigation of REE is very costly, computer modeling for analyzing and the engine alternative designing is more affordable. Farzaneh-Gord and Jannatabadi [15] modeled the single-acting REE and analyzed the effect of various parameters such as speed, port and piston diameter, connecting rod length and crank radius on the engine performance and proposed the optimized amount of these parameters. Farzaneh-Gord et al. [16] studied utilizing a REE at much lower pressure (between 4 and 17 bar) for Town Border pressure reduction Stations (TBS). In their study AGA8 equation of state has been used for calculating natural gas thermodynamic properties.

From the point of geometric and simulation view, a REE is similar to a reciprocating compressor. It just acts the reverse of compressor but instead of valves, spool valves are used for controlling inlet and outlet mass flow. Therefore, similar research on reciprocating compressors is worth reviewing. A lot of researches

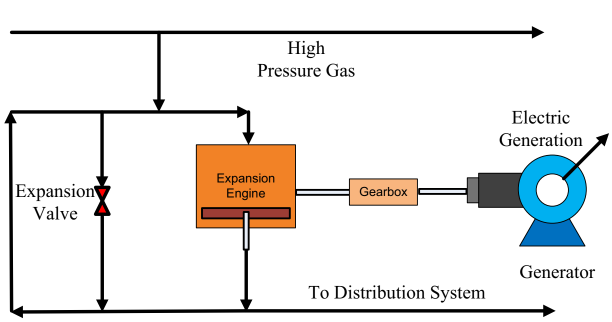

Fig. 1. A schematic diagram of installing an expansion engine in a CGS.

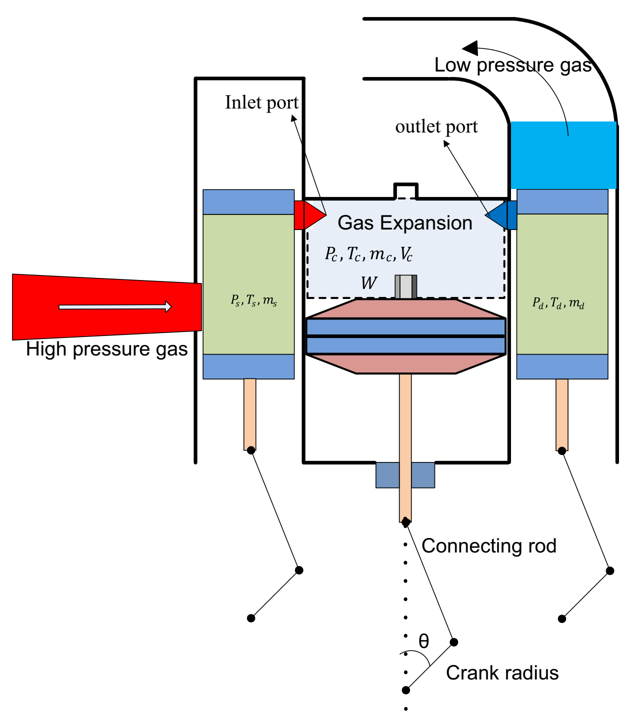

Fig. 2. A schematic diagram of a single acting reciprocating expansion engine.

have been reported on the further development of the methods of physical simulation and thermodynamic processes occurring on the reciprocating compressors to predict overall performance under various conditions [17–19]. One study investigates performance and volumetric efficiency of reciprocating compressors and introduces some parameters which cause decreasing the efficiency of the system [20]. In a theoretical simulation, based on real and ideal gas assumption, the effects of such important parameters has been analyzed on the performance of natural gas reciprocating compressor and results show that there is a difference between temperature, indicated work and mass flow rate of compressor when the gas is assumed to be ideal or real [21].

Since the physical resemblance of REE to the Spark Ignition (SI) engine or reciprocating compressor and the effect of ports opening and closing time on exergy destruction due to inlet/outlet throttling, the researches on exergy modeling of reciprocating compressor and SI engine are also worth presenting. Exergy analysis has been interested by researchers in recent years to predict the energy loss recourses of systems and to increase system performance. Studies such as [22–24,20] have been done on exergy analysis of natural gas during pressure reduction. The measurement of parameters which waste the compressor shaft power has been studied by McGovern [23]. He studies on the exergy destruction of reciprocating compressor due to heat transfer, friction, inlet/outlet throttling and mixing and identify their locations [25]. Study on the effects of some design and operating parameters on the exergy analysis of SI engine shows that changing these parameters have a huge effect on the irreversibility of engine during its process [26]. The type motion and geometry of valve is a basic parameter to control the mass flow rate. Semlistch studied on the valve and piston motion to investigate the energy loses of SI engine [27]. There are many styles of slide or piston valves to control mass flow of steam engines [28]. In this thesis two cylindrical valves are used for this purpose, Fig. 2.

A single valve reciprocating expander has been studied and it was shown that there is high flow speed due to pressure difference in admission process [29]. The main goal of the present study is to optimize the opening and closing time of inlet and outlet ports theoretically. Scientific researchers have not been carried out on the exergy analysis of REE yet. Since the first law analysis does not give enough information about the performance of a REE, the current study is based on minimizing entropy generation during suction, expansion, discharge and recompression processes. For this purpose a thermodynamic model has been developed. In this model, control volume is assumed as gas inside the cylinder (see Fig. 2). The model could predict in-cylinder pressure and temperature at various crank angles. Through the analysis, the effects CGS inlet pressure variation on exergy destruction has been investigated. The fluid flow through the inlet and outlet ports modeled as fluid flow through orifices. Genetic Algorithm is selected for optimization and second law efficiency is considered as fitness function. The number of population size is considered 20 and Roulette function is utilized for optimization. The continuity and first law of thermodynamic with heat transfer between the in-cylinder natural gas and environment are considered simultaneously to calculate the gas temperature and pressure. The natural gas is assumed as methane and modeled as an ideal gas.

2. First law thermodynamic

The first law for selected control volume (in-cylinder gas) could be presented as [30]:

$$\frac{dE_{CV}}{dt} = \dot{Q}_{CV} - \dot{W}_{CV} + \sum(\dot{m}h)_s - \sum(\dot{m}h)_d \tag{1}$$

It could be seen that the potential and kinetic energy are assumed negligible in inlet an outlet enthalpy fluxes. For inlet/outlet conditions the suction/discharge temperature and pressure are considered as boundary conditions. In Eq. (1), the work term could be calculated as [31]:

$$W_{CV} = \int_{\theta=0}^{\theta=360} P_c dV_c \tag{2}$$

The work obtained from the above equation should be considered as indicator work. It is assumed that the energy of system is a function of internal energy only, it means that potential and kinetic energy are negligible [32] which follows that:

$$\frac{dE_{CV}}{dt} = \frac{d(m_c u_c)}{dt} = m_c\frac{du_c}{dt} + u_c\frac{dm_c}{dt} \tag{3}$$

Heat transfer between in-cylinder gas and ambient could be modeled as follow [32].

$$\dot{Q}_{CV} = U(t)A(t)(T_a - T_c(t)) \tag{4}$$

$U(t)$ and $A(t)$ are overall heat transfer coefficient and instantaneous heat transfer area, respectively. The more information about heat transfer modeling could be found in [33]. The mass conservation law could be expressed as [31]:

$$\frac{dm_c}{dt} = \frac{dm_s}{dt} - \frac{dm_d}{dt} \tag{5}$$

With substituting the Eqs. (4) and (5) in Eq. (1), the following equation could be obtained [32]:

$$\frac{du_c}{dt} = \frac{1}{m_c}\left(U(t)A(t)(T_a - T_c(t)) - P_c\frac{dV_c}{dt} + \dot{m}_s h_s - \dot{m}_d h_c - \dot{m}_c u_c\right) \tag{6}$$

The above equations are differentiated respect to time, to convert them to the form of crank angle, the following equation could be used [32]:

$$\frac{d}{dt} = \frac{d}{d\theta}\frac{d\theta}{dt} = \omega\frac{d}{d\theta} \tag{7}$$

where ω is the rotational speed of crank shaft. Since for ideal gas $du_c = C_v dT_c$, the first law of thermodynamic could be rearranged as below [32]:

$$\frac{dT_c}{d\theta} = \frac{1}{m_c C_v}\left(\frac{1}{\omega}U(t)A(t)(T_a - T_c(t)) - P_c\frac{dV_c}{d\theta} + \frac{dm_s}{d\theta}h_s - \frac{dm_d}{d\theta}h_c - u_c\left(\frac{dm_s}{d\theta} - \frac{dm_d}{d\theta}\right)\right) \tag{8}$$

For calculating instantaneous pressure and temperature of gas as a function of crank angle, each degree is divided into 10 steps; it means that 3600 steps are used to mathematical simulation convergence. The difference between the initial and final in-cycle temperature and pressure is considered as a convergence function. Then based on Euler method and ideal gas equation of state temperature and pressure of gas could be calculated as follow [15]:

$$T_c^{j+1} = T_c^j + dT_c^j \tag{9}$$

$$P_c^{j+1} = \frac{m_c^{j+1} R_g T_c^{j+1}}{V_c^{j+1}} \tag{10}$$

3. Thermodynamic properties calculation

In this study, the specific heat capacity of methane is considered as a function of temperature as follow [34]:

$$\begin{gathered} C_P(T) = A_1 + B_1\left[\frac{C_1/T}{\sinh(C_1/T)}\right]^2 + D_1\left[\frac{E_1/T}{\cosh(E_1/T)}\right]^2 \\ A_1 = 3.3298\times10^4,\quad B_1 = 7.9933\times10^4,\quad C_1 = 2.0869\times10^3, \\ D_1 = 4.1602\times10^4,\quad E_1 = 9.9196\times10^2 \end{gathered} \tag{11}$$

For calculating the enthalpy of methane, the below equation could be used [34]:

$$h(T) = h_{id} + A_1(T - T_0) + B_1C_1\left[\coth\left(\frac{C_1}{T}\right) - \coth\left(\frac{C_1}{T_0}\right)\right] - D_1E_1\left[\tanh\left(\frac{E_1}{T}\right) - \tanh\left(\frac{E_1}{T_0}\right)\right] \quad (12)$$

And then the internal energy could be calculated as [30]:

$$u(T) = h(T) - R_gT \quad (13)$$

Entropy of methane could be calculated as [34]:

$$s(T,P) = s_{id} + s(T) - R_g\ln\left(\frac{P}{P_0}\right) \quad (14)$$

where [34]:

$$s(T) = A_1\ln\left(\frac{T}{T_0}\right) + B_1\left[\left(\frac{C_1}{T}\right)\coth\left(\frac{C_1}{T}\right) - \left(\frac{C_1}{T_0}\right)\coth\left(\frac{C_1}{T_0}\right) - \ln\left(\sinh\left(\frac{C_1}{T}\right)\right) + \ln\left(\sinh\left(\frac{C_1}{T_0}\right)\right)\right] - D_1\left[\left(\frac{E_1}{T}\right)\tanh\left(\frac{E_1}{T}\right) - \left(\frac{E_1}{T_0}\right)\tanh\left(\frac{E_1}{T_0}\right) - \ln\left(\cosh\left(\frac{E_1}{T}\right)\right) + \ln\left(\cosh\left(\frac{E_1}{T_0}\right)\right)\right] \quad (15)$$

4. Geometrical modeling

According to slider crank mechanism, the piston instantaneous position could be calculated as [15]:

$$x(\theta) = x_0 + R(1-\cos\theta) + L\left\{1 - \sqrt{1 - \left(\frac{R}{L}\right)^2 \sin^2\theta}\right\} \quad (16)$$

where x_0 is the length of clearance volume. Then the cylinder volume will be calculated as [15]:

$$V_c(\theta) = x(\theta)\pi\frac{D_i^2}{4} \quad (17)$$

5. Mass flow rate modeling

The inlet/exhaust port timing is one of the most important parameters which has a major effect on the engine performance and is controlled by a spool valve, Fig. 2. Here, it is assumed that two spool valves are being employed to control inlet and outlet mass flow. This gives a freedom for selecting optimized period of opening of each inlet/outlet ports. Instantaneous inlet and outlet ports cross sectional area are modeled with a sine function as follows [15]:

$$\frac{dm_s}{d\theta} = \begin{cases} \frac{1}{\omega}A_sP_s\sin\left(\frac{\theta}{\theta_0}\pi\right)\sqrt{\frac{2\gamma}{(\gamma-1)R_gT_s}}\sqrt{\left(\frac{P_c}{P_s}\right)^{\frac{2}{\gamma}} - \left(\frac{P_c}{P_s}\right)^{\frac{\gamma+1}{\gamma}}} & \text{if } \frac{P_c}{P_s} > \left(\frac{2}{\gamma+1}\right)^{\frac{\gamma}{\gamma-1}} \\ \frac{1}{\omega}A_sP_s\sin\left(\frac{\theta}{\theta_0}\pi\right)\sqrt{\frac{\gamma}{R_gT_s}\left(\frac{2}{\gamma+1}\right)^{\frac{\gamma+1}{\gamma-1}}} & \text{if } \frac{P_c}{P_s} \leqslant \left(\frac{2}{\gamma+1}\right)^{\frac{\gamma}{\gamma-1}} \end{cases} \quad (18)$$

$$\frac{dm_d}{d\theta} = \begin{cases} \frac{1}{\omega}A_dP_c\sin\left(\frac{\theta-\theta_i}{\theta_e-\theta_i}\pi\right)\sqrt{\frac{2\gamma}{(\gamma-1)R_gT_c}}\sqrt{\left(\frac{P_d}{P_c}\right)^{\frac{2}{\gamma}} - \left(\frac{P_d}{P_c}\right)^{\frac{\gamma+1}{\gamma}}} & \text{if } \frac{P_d}{P_c} > \left(\frac{2}{\gamma+1}\right)^{\frac{\gamma}{\gamma-1}} \\ \frac{1}{\omega}A_dP_c\sin\left(\frac{\theta-\theta_i}{\theta_e-\theta_i}\pi\right)\sqrt{\frac{\gamma}{R_gT_c}\left(\frac{2}{\gamma+1}\right)^{\frac{\gamma+1}{\gamma-1}}} & \text{if } \frac{P_d}{P_c} \leqslant \left(\frac{2}{\gamma+1}\right)^{\frac{\gamma}{\gamma-1}} \end{cases} \quad (19)$$

It could be realized that based on gas dynamic law, the chocking in the ports occurs when the pressure ratio is less than $(2/(\gamma+1))^{\gamma/\gamma-1}$.During the chocking, the port mass flow rate should be calculated using the relation in the bottom of Eqs. (18) and (19) [14]. In these equations θ_0 is intake port closure timing (IPCT), θ_i is an exhaust port opening timing (EPOT), and θ_e is an exhaust port closure timing (EPCT) (see Fig. 3).

6. Exergy analysis

Exergy of a system is the maximum work which could be achieved if the system is brought to equilibrium with the environment. Exergy cannot be created but it can be destroyed due to thermodynamic irreversibility such as friction, mixing, heat transfer and throttling.

According to Kotas, exergy efficiency is defined as the ratio of the "desired exergy output" to the "exergy used" [35]. Tsatsoron is prefers the terms "product" and "fuel" instead, respectively [36]. The meaning of "desired exergy effect" or "product" is the desired result produced in the system whereas the "exergy used" or "fuel" defines as the net resources to produce the desired effect [37]. Eventually, it is preferable to say that, exergy efficiency is the ratio of "actual work developed by the system" and the "exergy made available to the system":

$$\Psi = \frac{B_{\text{actual work by the system}}}{B_{\text{exergy made to system}}} \quad (20)$$

In REE, actual work is the power generation or brake work and the exergy used to get this power is the different between total exergy input and output which is called exergy transfer. Then the ratio of brake work to exergy transfer is exergy efficiency as [38]:

$$\Psi = \frac{W_b}{\Xi_t} \quad (21)$$

$$W_b = W_{C.V} - W_f \quad (22)$$

For calculating the rate of exergy transfer to control volume, the inlet and outlet mass flow rates and thermodynamic properties of gas inside the control volume should be evaluated. The ambient temperature and suction/discharge conditions should be considered to calculate the inlet/outlet exergy. The rate of exergy transfer is given by [38]:

$$\dot{\Xi}_t = \dot{m}(b_s - b_d) = (\dot{m}_sh_s - \dot{m}_dh_d) - T_0(\dot{m}_ss_s - \dot{m}_ds_d) \quad (23)$$

Parameters causing the irreversibility within gas stream in expansion chamber are heat transfer between the gas and the

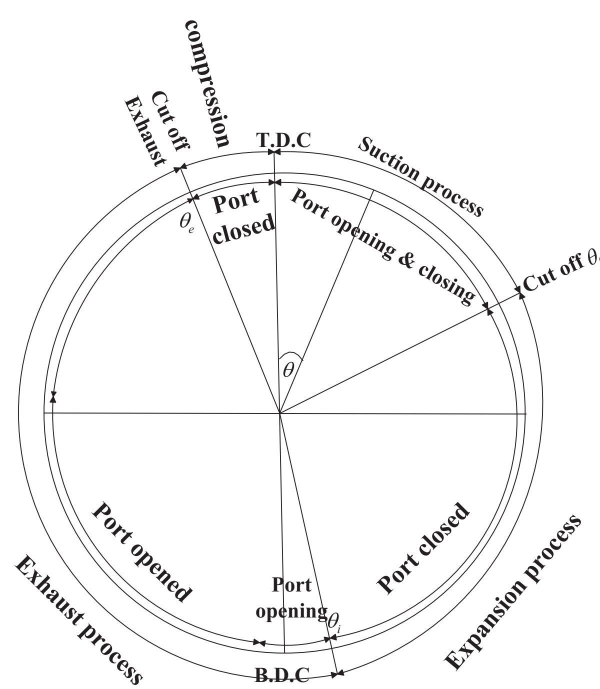

Fig. 3. Timing of expansion engine.

ambient, mixing of inlet stream, inlet/outlet throttling and friction. For calculating the heat transfer, two control volumes are assumed. First, the heat transfer between the ambient at temperature of T_a and the temperature of solid at T_w, and then heat transfer between the solid and the gas inside the expansion chamber by the temperature of T_c, (see Fig. 4). In this study, it is assumed that $T_w = T_{w,in} = T_{w,out} = (T_s + T_d)/2$ [32]. In REE due to long period of discharge process, discharge temperature could not considered constant. Consequently, it is calculated as:

$$T_d = \frac{\sum(m_d T_c)}{\sum m_d} \tag{24}$$

Hence the irreversibility due to heat transfer from an ambient to the gas is given by [38]:

$$\dot{I}_Q = T_0\left[\dot{Q}_{in}\left(\frac{1}{T_c} - \frac{1}{T_w}\right) + \dot{Q}_{out}\left(\frac{1}{T_w} - \frac{1}{T_a}\right)\right] \tag{25}$$

The process of inlet/outlet throttling was assumed as an adiabatic and isenthalpic process. Irreversibility due to these throttling could be computed as [35]:

$$\dot{I}_{th_i} = T_0 \dot{m}_s [s_c - s_i] \tag{26}$$

$$\dot{I}_{th_e} = T_0 \dot{m}_d [s_d - s_c] \tag{27}$$

where s_i and s_d are entropy at the suction line and discharge condition respectively.

Since, there is a temperature difference between the inlet gas and in-cylinder gas, there would be another irreversibility due to mixing which is calculated as follows [25]:

$$\begin{aligned}\dot{I}_{mix} &= \dot{m}_s T_0\left[(s_c - s_i) - \frac{h_c - h_s}{T_c}\right] \\ &= \dot{m}_s T_0 C_p\left(\ln\left(\frac{T_c}{T_s}\right) - \frac{T_c - T_s}{T_c}\right)\end{aligned} \tag{28}$$

Considering oil free piston ring, friction work due to piston movement of expansion engine could be calculated as below [39]:

$$W_f = 2S\pi f P_c L_r D_i \tag{29}$$

L_r is the ring width, S is stroke length, f is the friction coefficient of PTFE and P_c is the in-cylinder gas pressure.

7. Results and discussion

Energy and exergy analyses as well as optimization based on minimizing exergy destruction or maximizing exergy efficiency are studied for a REE where the methane is considered as an ideal gas. For calculating the gas temperature and pressure, the first law of thermodynamic and the ideal gas state equation are used simultaneously. Inlet temperature, inlet and outlet pressure of in-cylinder gas should be specified at the beginning of the simulation. The equations which were described in the previous section are solved at each time-step to calculate thermodynamic properties of the gas. At the start of the cycle, the port is opened to admit gas into the cylinder. It closes to allow the gas to expand as the piston moves down the cylinder. Then it opens to release the low pressure gas from the cylinder and finally closes to compress the small amount of gas that remains in the cylinder before the cycle begins again. Thus, the ports are opened and closed in turn, twice in each cycle.

Firstly, to validate the numerical method, a comparison has been carried out between numerical, theoretical and measured values. The measured value has been reported in Ref. [40] for a steam engine. It should be pointed out that a steam engine could be considered as a REE. For validation, pressure–volume change has been compared. For this purpose a uni-flow configuration of steam engine is compared with REE. In uni-flow configuration exhaust ports are located on cylinder wall, it means that piston controls the exhaust mass flow rate. In this comparison case inlet pressure and temperature are assumed as 69 bar and 811 K, discharge pressure as 1.4 bar, piston diameter as 8.9 cm, motor speed as 2000 rpm, inlet port diameter as 1.9 cm, five valve square with sides of 1 cm and stroke of 9 cm. Fig. 5 shows the comparison. As it could be realized there is a good agreement between the numerical and measured values.

The calculations are performed for the inlet pressures of 70 and 55 bars. Optimum opening and closing time of the ports is calculated in order to maximize exergy efficiency. In optimization with Genetic Algorithm, 700 iterations are carried out to reach the best timing. Then by considering the piston average speed and piston diameter, other aspects of engine have been optimized respect to these values. Table 1 shows the major components of a piston engine.

At first, for optimization, a basic case of engine geometry is considered, $D_i = 16$, $D_o = 18$, $d_s = d_d = 5$, $S = 2R = 14$, $L = 20$ cm and $CL = 7\%$. From these values, it could be realized that piston diameter is larger than piston stroke which develops greater peak power.

In expansion engines, average piston speed should be between 3.2 and 4.4 m/s [41]. From equation of $u_{ave} = 2SN$ and $S = 2R$, this leads to change crank radius from 6.4 to 8.8 cm. Here, in basic case crank radius of 7 cm with average piston speed of 3.5 m/s is assumed. Then due to the dimensions, Table 1, based on average

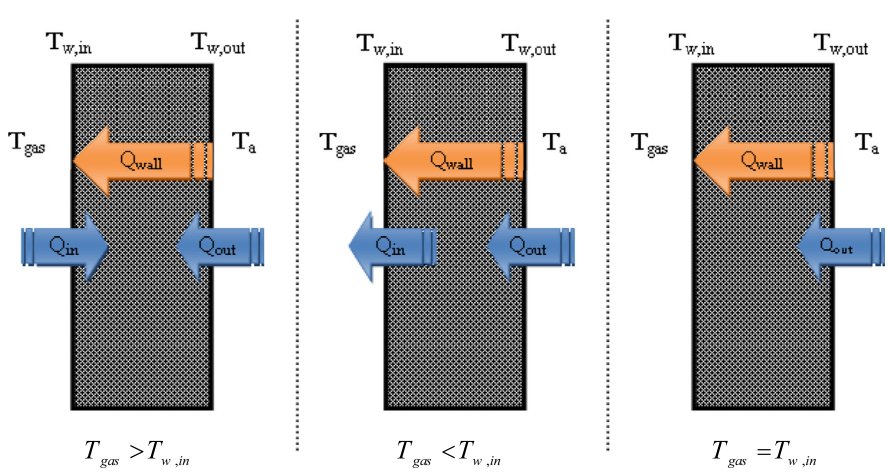

Fig. 4. Heat transfer between ambient and gas.

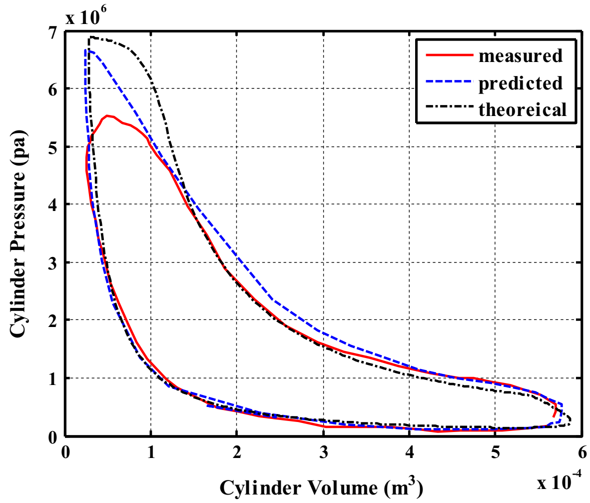

Fig. 5. Comparison between numerical and theoretical–experimental values of steam engine.

Table 1
Physical parameters of studied expansion engine.

Operating condition	Data	Operating condition	Data
P_s	55 and 70 bars	D_i	14.6–16–18.3–20.1 cm
P_d	17 bars	$D_o/D_i = 1.125$	16.4–18–20.6–22.6 cm
$d_s/D_i = 0.3125$	4.6–5–5.7–6.3 cm	T_s	300 K
$d_d/D_i = 0.3125$	4.6–5–5.7–6.3 cm	T_a	298 K
V_0	7% V_{dis}	f	0.2
L_r	0.5 cm	$2R/D_i = 0.875$	6.4–7–8–8.8 cm
N	750 rpm	$L/D_i = 1.25$	18.3–20–22.9–25.1 cm

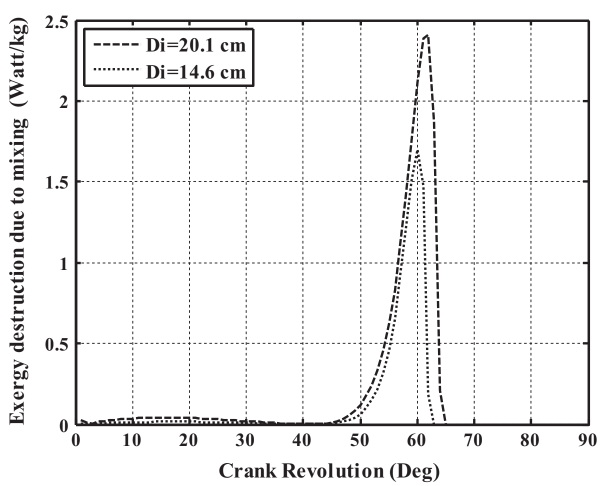

Fig. 6. Exergy destruction due to mixing.

piston speed of 3.2, 4 and 4.4 m/s, crank radius is selected as 6.4, 8 and 8.8 cm, respectively. In general, a total of 8 various engine dimensions have been studied. It should be pointed out that basic case is selected after the optimized timing was obtained for various cases. Consequently, the basic case may have the optimum parameters.

7.1. Selecting the basic case of engine geometry based on optimum exergy efficiency

To optimize the inlet/outlet ports opening and closing time, at first, a basic case is selected for REE geometric, see Table 1, and

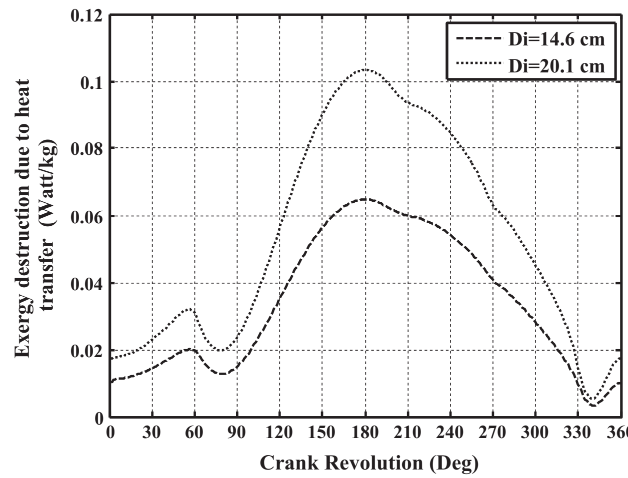

Fig. 7. Exergy destruction due to heat transfer.

case 2, which piston diameter is 16 cm, port diameters are 5 cm, crank radius is 7 cm and connecting rod is 20 cm. It will be proved later, based on the results, that these selected dimensions are very close to optimum values. At first, it should be noted that exergy destruction due to mixing and heat transfer in all cases is so small that they can be neglected; (see Figs. 6 and 7). It should be also point out that with increasing the engine size exergy destruction due to mixing and heat transfer will increase.

In Fig. 8, it can be realized that with inlet port diameter variation from 2 to 6 cm while the diameter of the outlet port kept constant at 5 cm, exergy efficiency increases because of increasing mass flow rate. Figs. 9 and 10 show that with increasing inlet port diameter, exergy destruction due to inlet/outlet throttling will be decrease. Since the effect of port diameter of 5 and 6 cm is very close, due to geometric constraints of larger port area tends to increase the clearance volume which may have a negative effect on efficiency; consequently port diameter of 5 cm is selected as an optimum basic case. Smaller port does not have selected because it can be seen that the exergy efficiency will be smaller in these values, and consequently output power of REE will be smaller too. For example in port diameter of 2 cm, the amount of power generation achieved almost 1914 kW/kg, although with port diameter of 5 cm, REE will be produced 2277 kW/kg of power. With variation of port diameter, exergy destruction due to friction is varied from 4.7 to 5.7 kW.

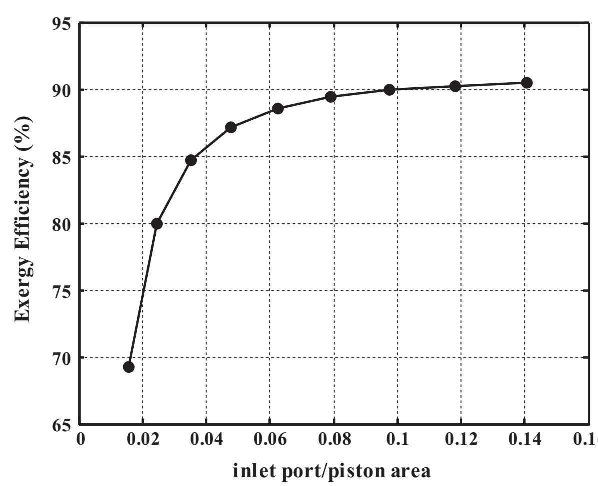

Fig. 8. Effect of inlet port diameter on exergy efficiency.

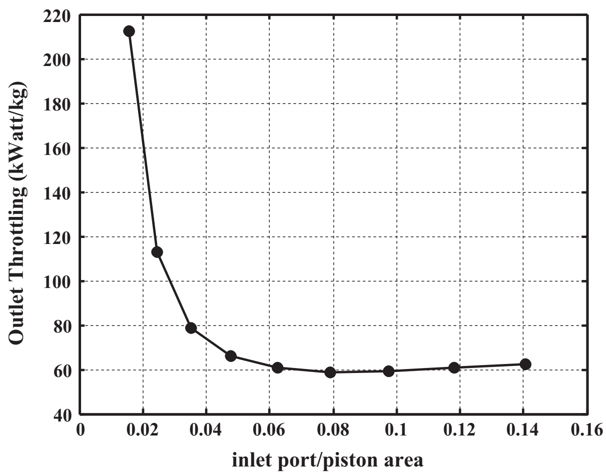

Fig. 9. Effect of inlet port diameter on outlet throttling.

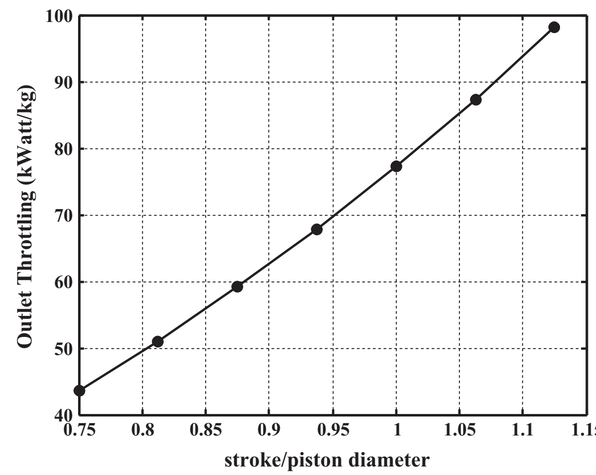

Fig. 12. Effect of piston stroke on outlet throttling.

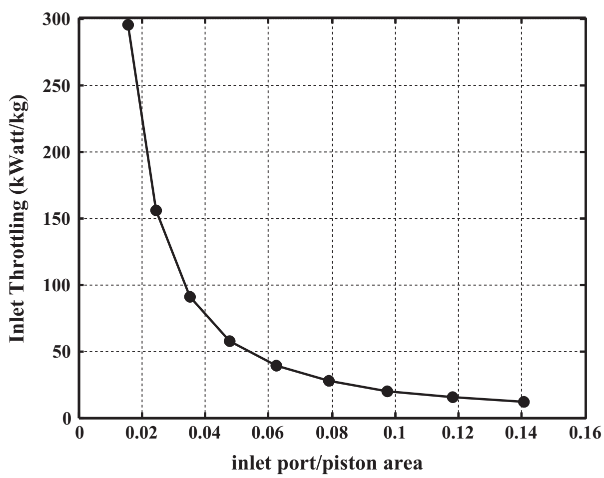

Fig. 10. Effect of inlet port diameter on inlet throttling.

Fig. 11 shows that crank radius variations from 6 to 9 cm causes a reduction in the exergy efficiency from about 91–87%. So it could be concluded that increasing the piston stroke causes that the exergy transfer to raise more sharply comparing with brake power. Consequently, it is preferable to select a small crank radius or a small piston stroke. Since that the minimum average piston speed is assumed as 3.2 m/s, value of 6 cm for crank radius is not suitable and then it is selected as 7 cm for the basic case of geometry. Figs. 12 and 13 show that increasing piston stroke will be resulted to increase in exergy destruction. This is due to inlet and outlet throttling. These figures show that for a typical engine size, exergy destruction due to outlet throttling is higher than inlet throttling. As an example in a basic geometrical case, 60 kW/kg exergy will be destroyed when gas pass through outlet port, whereas 20 kW/kg will be destroyed through inlet port.

From Fig. 14, it could be realized that exergy efficiency is not much affected by variation of connecting rod length from 15 to 35 cm; therefore, the value of 20 cm is selected as a basic case of connecting rod, although values more than 20 cm could be also selected. Figs. 15 and 16 show that selecting the basic value of connecting rod length is not very important, because of its low impact on exergy destruction. Based on outlet throttling connecting rod length with more or equal than 20 cm is preferable than lower values, but according to inlet throttling, value of 20 cm has minimum exergy destruction. Friction power has not been affected much with variation of connecting rod length.

Piston cannot go and touch the extreme end of the cylinder at top dead center (TDC) position. A small volume between piston and end of the cylinder in addition the volume of port is called

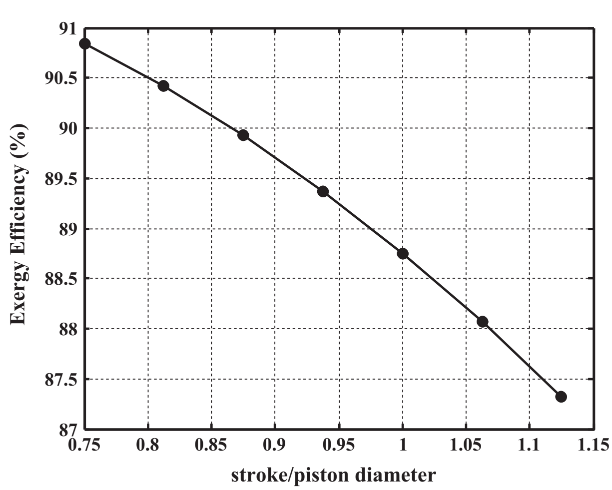

Fig. 11. Effect of stroke on exergy destruction.

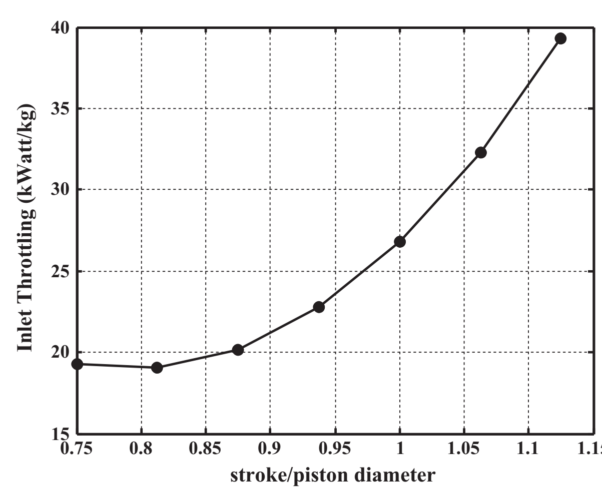

Fig. 13. Effect of piston stroke on outlet throttling.

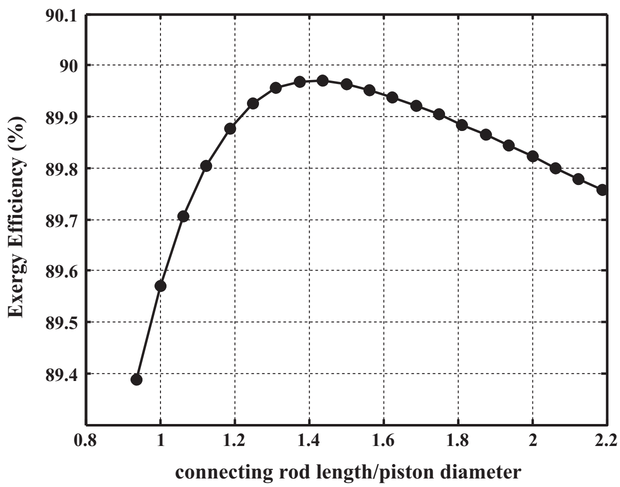

Fig. 14. Effect of connecting rod length on exergy efficiency.

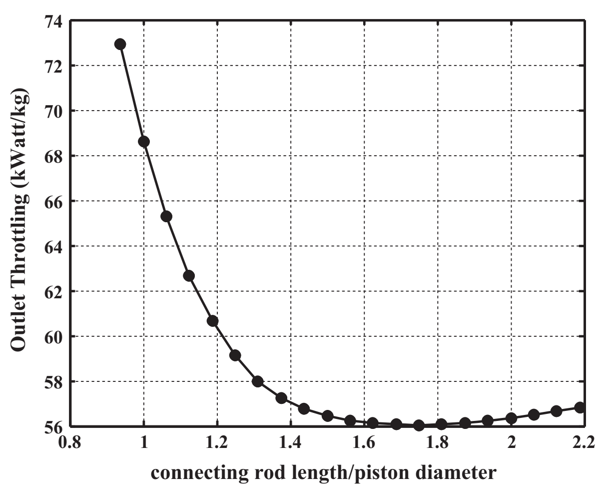

Fig. 15. Effect of connecting rod length on outlet throttling.

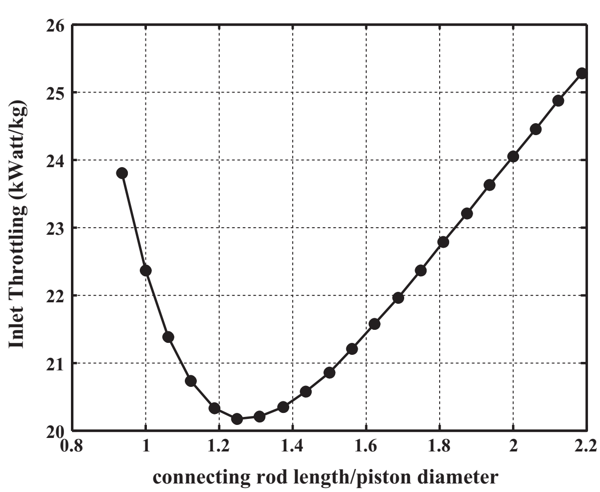

Fig. 16. Effect of connecting rod length on inlet throttling.

as the clearance volume. By varying the clearance volume from 5% to 15%, the optimum power and efficiency are achieved in the amount of 7%, (see Figs. 17 and 18). From Fig. 18 it can be seen that 2270 kW/kg power is generated in 7% of clearance volume which is

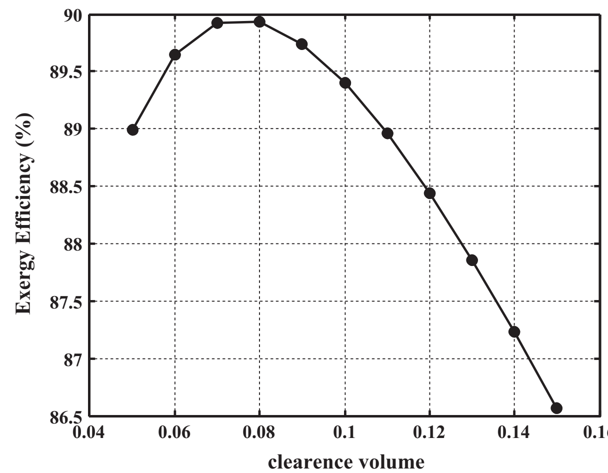

Fig. 17. Effect of clearance volume on exergy efficiency.

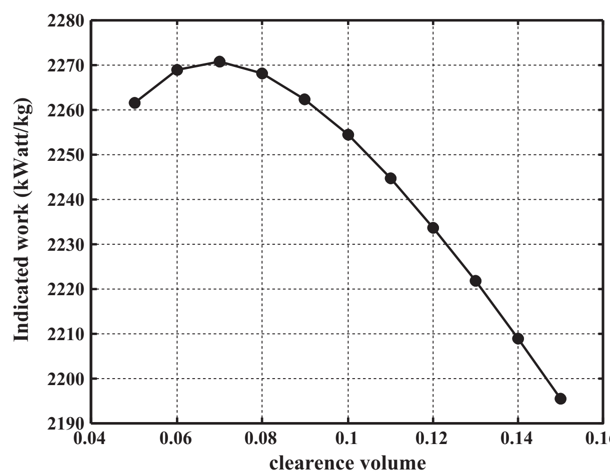

Fig. 18. Effect of clearance volume on indicated power.

more than other values. Although the effect of clearance volume on exergy efficiency is very little so that it changes from 89% to 90% between 5% and 7%. Then for all REE cases this value is selected for clearance volume.

7.2. Results of port optimum timing (opening and closing time)

Based on above discussions, Table 2 shows the results of optimum opening and closing time of ports in every case of engines. For optimization it was assumed that there is no back flow from inside cylinder to suction line and from discharge line to inside cylinder. With this constraint as it can be seen from Table 2, by reducing the inlet pressure condition from 70 to 55 bars, IPCT is

Table 2
Optimum opening & closing time of ports for several engines.

	P_s	T_s	D_i	d_s	S	L	θ_0	θ_i	θ_e
Case 1	70	300	14.6	4.6	12.8	18.3	62	198	330
Case 2	70	300	16	5	14	20	63	194	331
Case 3	70	300	18.3	5.7	16	22.9	63	197	332
Case 4	70	300	20.1	6.3	17.6	25.1	64	194	333
Case 5	55	300	14.6	4.6	12.8	18.3	70	206	335
Case 6	55	300	16	5	14	20	72	193	336
Case 7	55	300	18.3	5.7	16	22.9	72	198	337
Case 8	55	300	20.1	6.3	17.6	25.1	72	202	337

associated with a slight delay, from an average angle of 63° to an angle of 72°, due to having same mass flow rate, suction process with inlet pressure of 55 bars should take longer than inlet pressure of 70 bars. EPOT in all cases is almost the same. Like IPCT, EPCT at inlet pressure of 55 bars has a further delay toward inlet pressure of 70 bars.

Table 2 shows that in the same inlet pressure and temperature condition, larger engine size almost does not have an effect on IPCT and EPCT. For example in case 1 to case 4 it can be seen that IPCT is about 63 and EPCT is 330–333° of crank revolution. It is interesting to note that the best time for beginning of discharge process, EPOT, is at upward piston movement from BDC to TDC. Generally, it could be said that changing engine size does not affect on optimization timing of REE. It means that for having less exergy destruction, discharge process should start after BDC. Also, it could be said that with selecting a larger REE, opening/closing timing of ports does not change significantly.

7.3. The effect of engine size on power generation and exergy efficiency

Fig. 19 shows that with increasing the engine size, exergy efficiency will increase very slightly so that it can be said that changing engine size does not affect on exergy efficiency of REE. The ratio of indicated power to total inlet mass flow rate does not change much and it has a short decline, (see Fig. 21). Figs. 21 and 22 also show that increasing mass flow rate and pressure ratio has a significant effect on amount of power generation. This is because of having a larger port diameter and therefore a more exergy destruction due to inlet/outlet throttling. From Fig. 20, it could be found that for various pressure ratios, optimization has been taken at constant mass flow rate in each engine size.

Fig. 22 shows that increasing piston diameter from 14.6 to 20.1 cm has a small effect on friction power of REE. Although with increasing inlet pressure, exergy destruction due to friction will increase too. In all cases, the portion of friction power is 5–15% of indicated power.

7.4. The effect of variation of inlet pressure

In CGS, the inlet pressure are varying during year but here the REE is optimized for a constant inlet pressure and then effects of inlet pressure variation are studied. Figs. 23 and 24 show that if optimization is done based on working pressure of 70 bars, inlet pressure should be kept above 30 bars, as for lower inlet pressure, the engine has a very small efficiency and it cannot generate power. This is basically due to high friction power comparing to indicator power. It means that in designing of REE with inlet pressure of 70 bars, if the inlet pressure drops to 30 bars, natural gas

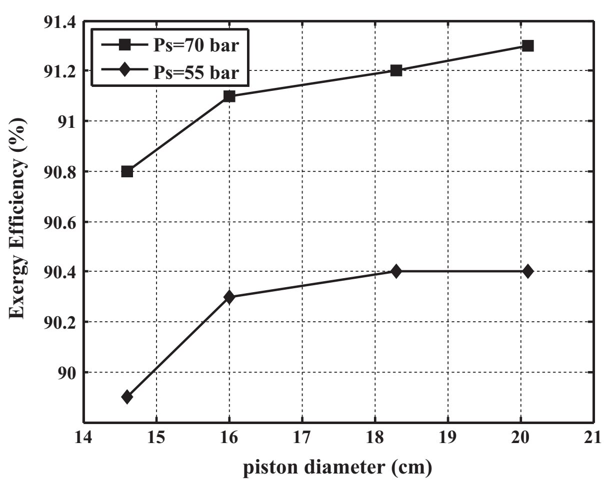

Fig. 19. Exergy efficiency of all engine.

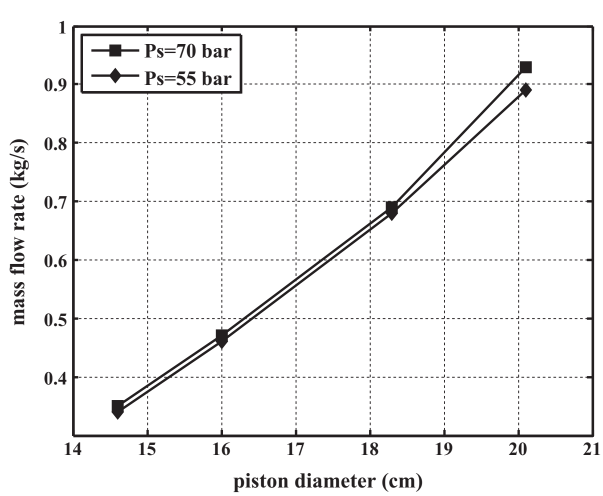

Fig. 20. Mass flow rate of all engine.

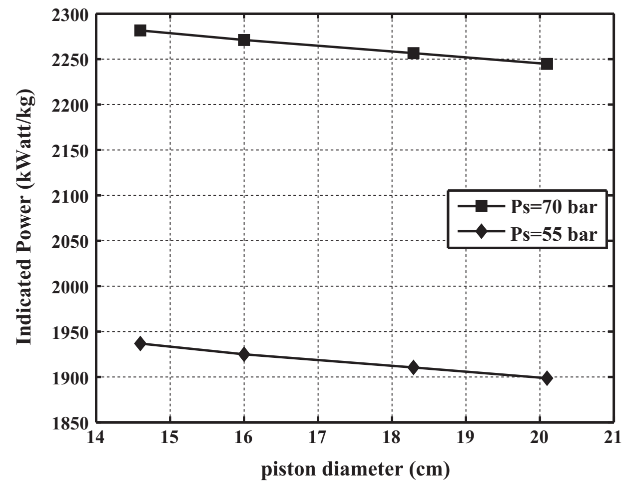

Fig. 21. Indicator power of all engine.

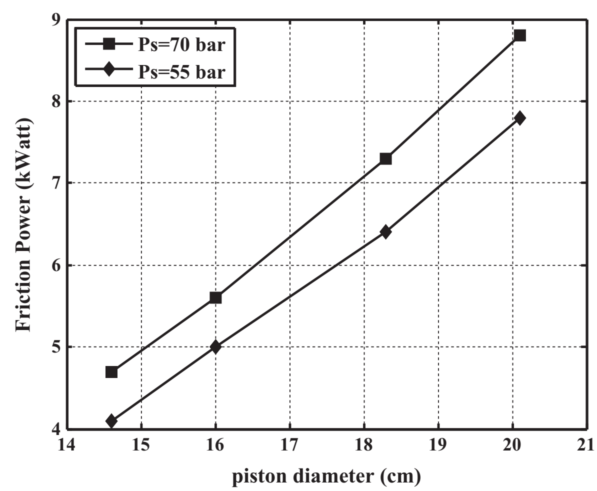

Fig. 22. Friction power of all engine.

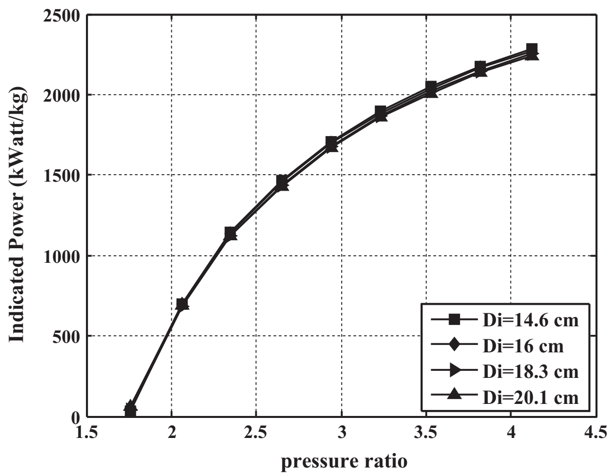

Fig. 23. Indicator power, pressure of 70 bars.

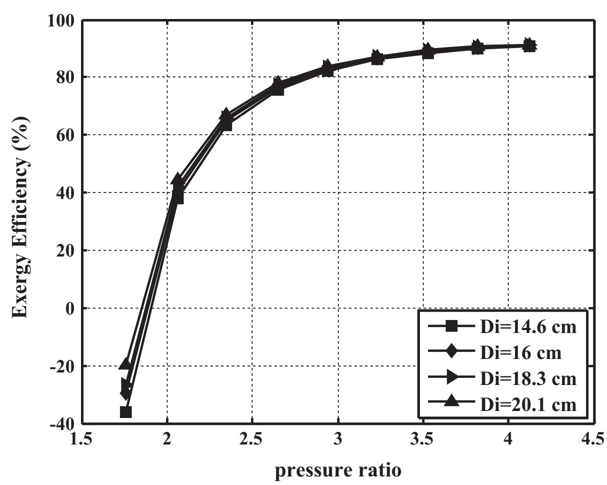

Fig. 24. Exergy efficiency, pressure of 70 bars.

should be passed through expansion valve instead of REE. In optimization based on working inlet pressure of 55 bars, for all pressure ratios, REE will produce electricity, (see Figs. 25 and 26).

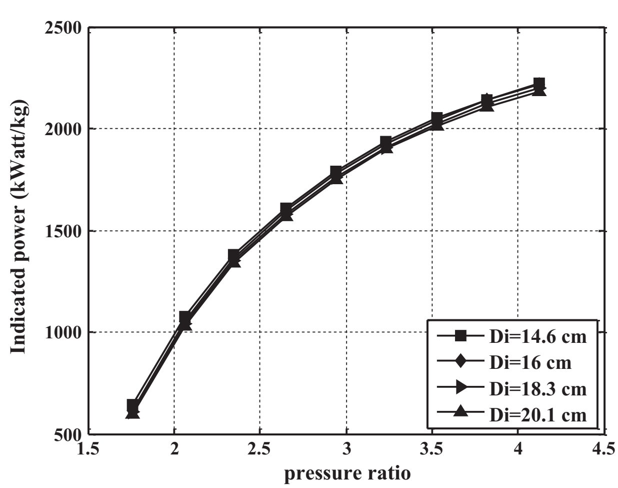

Fig. 25. Indicator power, pressure of 55 bars.

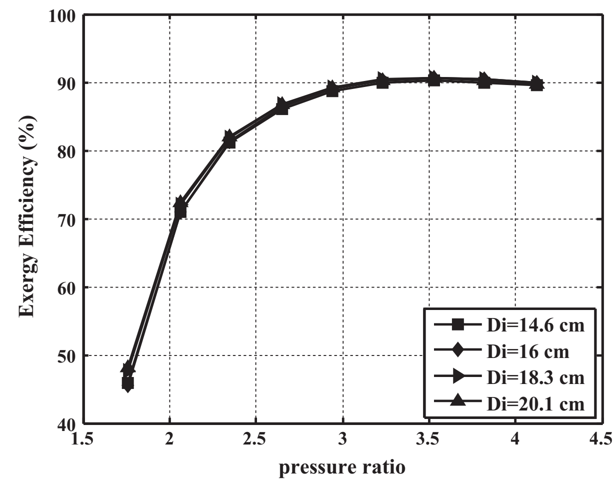

Fig. 26. Exergy efficiency, pressure of 55 bars.

Comparing Figs. 23 and 25, it could be realized that for timing optimization based on 55 bars, in low pressure ratios, designing with working pressure of 55 bars produces more power than pressure of 70 bars. By comparing Figs. 23 and 25, one could realize that in low pressure ratios, exergy destruction for inlet pressure of 70 bars is more than 55 bars and this behavior in high pressure ratios is reversed.

7.5. The effect of pressure ratio on exergy destruction resources

Results show that apart from friction which has the greatest effect on thorough exergy loss, the most part of exergy destruction occurs at discharge process, and exergy destruction due to mixing and heat transfer is very small. From Figs. 27–30 it could be realized that larger engine has more exergy destruction in both suction and discharge process. Figs. 27 and 28 show that in optimization with inlet pressure of 70 bars, there is more exergy destruction due to inlet and outlet throttling when the inlet pressure lower than the designed value (70 bars). But in optimization with inlet pressure of 55 bars, in both lower and higher pressure the amount of exergy destruction is more than inlet pressure of 55 bars, Figs. 29 and 30.

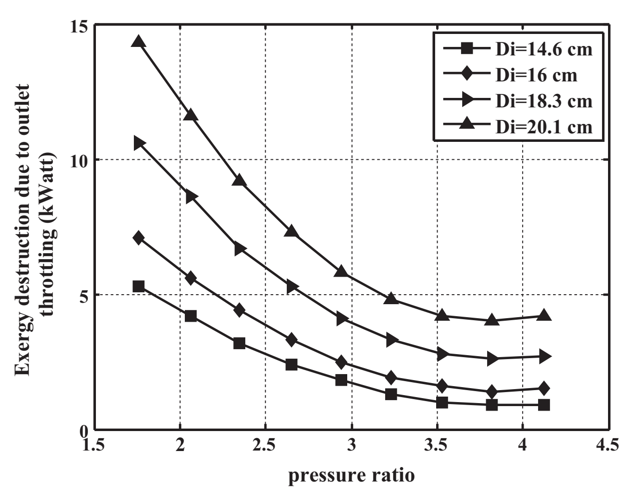

Fig. 27. Outlet exergy lost, pressure of 70 bars.

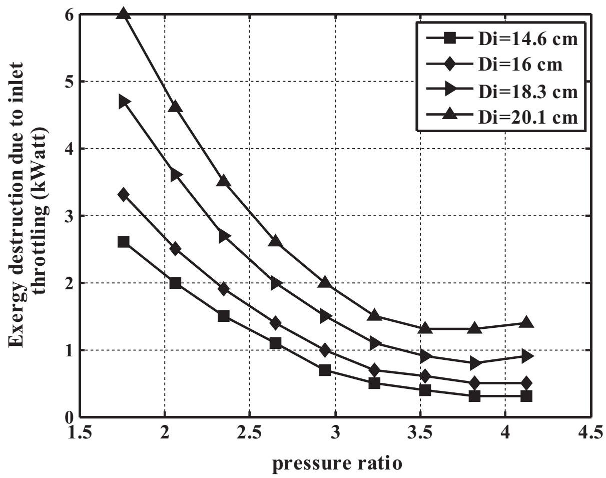

Fig. 28. Inlet exergy lost, pressure of 70 bars.

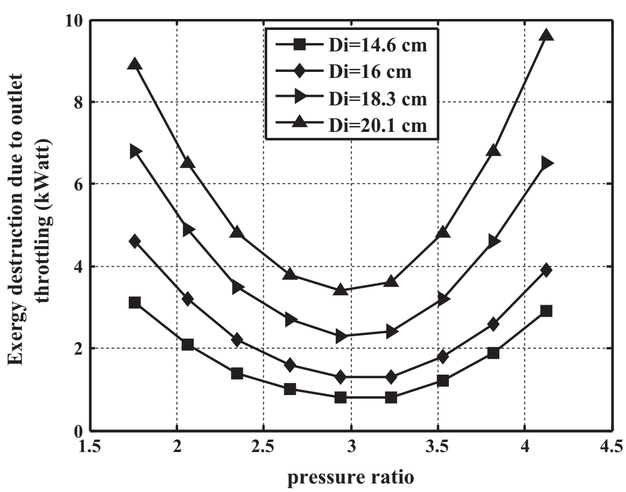

Fig. 29. Outlet exergy lost, pressure of 55 bars.

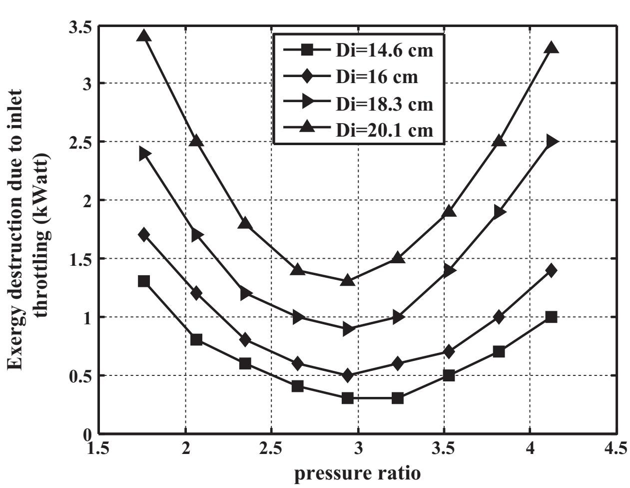

Fig. 30. Inlet exergy lost, pressure of 55 bars.

8. Conclusion

Optimization of exergy efficiency based on closing and opening time of ports besides effects of geometrical parameters has been carried out to study the REE performance and define the exergy destruction resources. On study of the geometrical effects, outlet port was kept constant at 5 cm. Then, the influences of the pressure ratio of the REE on the exergy efficiency and output power were investigated. Based on the results, the following conclusions could be made:

1- According to optimum angles calculated, selecting a small value of inlet port diameter and crank radius cause more exergy destruction due to throttling. But other parameters such as clearance volume and connecting rod length have less effective on thorough exergy loss.
2- The inlet/outlet ports opening and closing timing is an effective parameter on the rate of exergy destruction.
3- Mixing and heat transfer have a little effect on the rate of exergy destruction. For example in one case in 60 kW/kg exergy destruction, only 2.5 W/kg and 0.12 W/kg of exergy will be lost due to mixing and heat transfer respectively.
4- In all cases, the largest exergy destruction rates occurred due to friction and outlet throttling, respectively. In all cases a portion of 5–15% of exergy is destroyed due to friction. Exergy destruction due to outlet throttling is almost two times of exergy destruction due to inlet throttling.

Also, it could be concluded that the essential part of the exergy destruction from the single stage expansion engine is due to inlet and outlet throttling. As a result, proper timing of opening and closing ports is very influential in reducing the amount of exergy destruction.

Acknowledgment

The study was funded by the Gas Authority of Golestan. The authors would like to thank them for their sponsorship.

References

[1] Sanaye S, Nasab A. Modeling and optimization of a natural gas pressure reduction station to produce electricity using genetic algorithm. Selected topics in energy, environment, sustainable development and landscaping.
[2] Querol E, Gonzalez-Regueral B, García-Torrent J, Ramos A. Available power generation cycles to be coupled with the liquid natural gas (LNG) vaporization process in a Spanish LNG terminal. Appl Energy 2011;88:2382–90.
[3] Neseli MA, Ozgener O, Ozgener L. Energy and exergy analysis of electricity generation from natural gas pressure reducing stations. Energy Convers Manage 2015;93:109–20.
[4] Andrei I, Valentin T, Cristina T, Niculae T. Recovery of wasted mechanical energy from the reduction of natural gas pressure. Proc Eng 2014;69:986–90.
[5] Farzaneh Gord M, Eftekhari H, Tvakkoli M. Using of natural gas pressure reducing station to produce power and refrigeneration. In: Sixth national energy; 2007.
[6] Farzaneh-Gord M, Dasht-bayaz MD. Recoverable energy in natural gas pressure drop stations: a case study of the Khangiran gas refinery. Energy Explor Exploit 2008;26:71–82.
[7] Kostowski WJ, Usón S. Comparative evaluation of a natural gas expansion plant integrated with an IC engine and an organic Rankine cycle. Energy Convers Manage 2013;75:509–16.
[8] Ahmadi P, Dincer I, Rosen MA. Exergo-environmental analysis of an integrated organic Rankine cycle for trigeneration. Energy Convers Manage 2012;64:447–53.
[9] Dai Y, Wang J, Gao L. Parametric optimization and comparative study of organic Rankine cycle (ORC) for low grade waste heat recovery. Energy Convers Manage 2009;50:576–82.
[10] Poživil J. Use of expansion turbines in natural gas pressure reduction stations. In: Acta Montanistica Slovaca; 2004.
[11] Rezaie N, Saffar-Avval M. Feasibility study of turbo expander installation in city gate station. In: The 25th international conference on efficiency, cost, optimization, simulation and environmental impact of energy systems. Peru; June 26–29, 2012.
[12] Howarda C, Oosthuizen P, Peppley B. An investigation of the performance of a hybrid turboexpander-fuel cell system for power recovery at natural gas pressure reduction stations. Appl Therm Eng 2011;31(13):2165–70.
[13] Arabkoohsar A, Farzaneh-Gord M, Deymi-Dashtebayaz M, Machado L, Koury R. A new design for natural gas pressure reduction points by employing a turbo expander and a solar heating set. Renew Energy 2015;81:239–50.

[14] Dehli M. Concepts of gas expansion at high temperature. In: MECC Maastricht. Netherland; 1997.
[15] Farzaneh-Gord M, Jannatabadi M. Simulation of single acting natural gas Reciprocating Expansion Engine based on ideal gas model. J Nat Gas Sci Eng 2014;21:669–79.
[16] Farzaneh-Gord M, Izadi S, Deymi-Dashtebayaz M, Pishbin SI. Optimizing natural gas reciprocating expansion engines for Town Border pressure reduction stations based on AGA8 equation of state. J Nat Gas Sci Eng 2015;26:6–17.
[17] Benson RS, Azim A, Ucer AS. Some further analysis of reciprocating compressors systems. In: 2nd compressor technology conference. Purdue University; July 1974.
[18] Xie G, Bansal P. Dynamic simulation model of a reciprocating compressor in a refrigerator. In: International compressor conference at Purdue. West Lafayette; 2000.
[19] Maclaren J, Tramschek A, Pastrana O, Sanjirtes A. Advances in numerical methods to solve the equations governing unsteady gas flow in reciprocating compressor systems. In: 3rd compressor technology conference. Purdue University; July 1976.
[20] Navarro E, Granryd E, Urchueguia J, Corberan J. A phenomenological model for analyzing reciprocating compressors. Int J Refrig 2007;30:1254–65.
[21] Farzaneh-Gord M, Niazmand A, Deymi-Dashtebayaz M, Rahbari H. Thermodynamic analysis of natural gas reciprocating compressors based on real and ideal gas models. Int J Refrig 2015;56:186–97.
[22] Farzaneh-Gord M, Magrebi J. Exergy of natural gas flow in Iran's natural gas fields. Int J Exergy 2009;6:131–42.
[23] Farzaneh-Gord M, Hashemi S, Sadi M. Energy destruction in Iran's natural gas pipe line network. Energy Explor Exploit 2007;25:1–10.
[24] Farzaneh-Gord M, Manzari M, Magrabi M, Hashemi S, Eftekhari H, Farokhi A. Using pressure exergy of natural gas in Bandar-Abbas refinery gas pressure drop station. In: The second international conference on modelling, simulation, and applied optimization. Abu Dhabi, UAE; March 24–27, 2007.
[25] McGovern JA, Harte S. An exergy method for compressor performance analysis. Int J Refreg 1995;18(6):421–33.
[26] Sezer I, Bilgin A. Exergy analysis of SI engines. Int J Exergy 2008;5(2):204–17.
[27] Semlitsch B, Wang Y, Mihăescu M. Flow effects due to valve and piston motion in an internal combustion engine exhaust port. Energy Convers Manage 2015;96:18–30.
[28] Douglas A, Kerr P. Principles of steam locomotive valve systems; April 27, 2011.
[29] Zhang X, Xu Y, Xu J, Xue H, Chen H. Study of a single-valve reciprocating expander. J Energy Inst 2015:1–14.
[30] Moran MJ, Shapiro HN. Fundamentals of engineering thermodynamics. 6th ed. Wiley; 2007. ISBN: 0471787353 ed..
[31] Moran MJ, Shapiro HN, Boettner DD, Bailey MB. Fundamentals of engineering thermodynamics. John Wiley & Sons, Inc.; 2007.
[32] Lee S. First law analysis of unsteady processes with application to charging process and a reciprocating compressor; 1983.
[33] Ardali E, Heybatian E. Energy regeneration in natural gas pressure reduction stations by use of gas turbo-expander; evaluation of available potential in Iran. In: 24th world gas conference. Buenos Aires, Argentina; 5–9 October 2009.
[34] DIPPR@ 801, Evaluated standard thermophysical property values. Design Institute for Physical Properties, Sponsored by AIChE; 2004.
[35] Kotas TJ. The exergy method of thermal plant analysis. London: Butterworths; 1985.
[36] Tsatsaronis G. Thermoeconomic analysis and optimization of energy systems. Prog Energy Combust Sci 1993;19(3):227–57.
[37] Ghannadzadeh A. Exergetic balances and analysis in a process simulator: a way to enhance process energy integration; 2012.
[38] McGovern J, Harte S. Computer simulation of exergy destruction withina reciprocating. In: International compressor engineering conference. Purdue; 1992.
[39] Hanlon P. Compressor handbook. vol. 754. McGraw-Hill; 2001.
[40] Eckard S, Brooks R. Design of reciprocating single cylinder expanders for steam; October 1973.
[41] Spilling Gas Expansion, info@spilling.de. <http://www.spilling.de> [Online].